Available online at www.sciencedirect.com
ScienceDirect
Journal of Nuclear Materials 372 (2008) 45–52
journal of nuclear materials
www.elsevier.com/locate/jnucmat

Structure of Kurdjumov–Sachs interfaces in simulations of a copper–niobium bilayer

M.J. Demkowicz *, R.G. Hoagland

Los Alamos National Laboratory, Los Alamos, NM 87545, USA

Received 27 September 2006; accepted 8 February 2007

Abstract

An interfacial atomic structure that contains a strained monolayer of copper is described for copper and niobium in the Kurdjumov–Sachs orientation relation. The interfacial monolayer accommodates the inherent misfit between the adjoining crystals. Computer simulations using embedded-atom potentials demonstrate that the improved coordination of interface atoms in this structure can offset the energy penalty associated with creating the strained Cu monolayer sufficiently to make this interface structure energetically favorable with respect to one created by simply joining two perfect Cu and Nb crystals. Insight gained from the analysis of this novel interface structure is applied to predicting what other pairs of materials may form interfaces that lead to improved radiation damage resistance, such as that observed in CuNb multilayer thin-film composites.

PACS: 68.35.−p; 61.72.Nn; 68.65.Ac; 61.82.Bg

1. Introduction

Experimental investigations have demonstrated that thin-film multilayer composites of Cu (fcc) and Nb (bcc) exhibit high thermal stability [1,2] as well as superior mechanical [3,4] and fatigue [5] properties not observed in bulk Cu or bulk Nb. Theoretical explanations of these properties rely on the behavior of crystal defects in material close to CuNb interfaces, which – for composites with layer thicknesses as small as 4 nm – makes up a significant volume fraction of the overall thin film. Further evidence for the crucial role played by interface regions is observed in the radiation damage-resistance of CuNb multilayer composites during high-dose implantations of 33 keV and 150 keV He^+ at room temperature [6] and at elevated temperatures [7]. The remarkable microstructural stability of the composites seen in these experiments suggests that CuNb interfaces are barriers to implantation-induced mixing, catalytic surfaces for rapid annihilation of Frenkel pairs created during energetic ion bombardment, sites for nucleation of nanometer-sized bubbles from the implanted He, and fast diffusion pathways for its subsequent escape from the composite. Because they posses such remarkable radiation damage resistance properties, CuNb composites – if manufactured in large quantities through processes such as cold drawing [8,9] – are attractive candidate structural materials for the next generation of nuclear reactors. Since, the selection of structural materials for these reactors will furthermore take into account factors such as corrosion resistance in specific environments as well as nuclear activation behavior, it is desirable to have the capability of predicting what other pairs of materials form interfaces that mitigate radiation damage as do the ones found in CuNb multilayer thin-film composites. The study presented here aims to build such predictive capability by studying the intimate atomic structure of interfaces between Cu and Nb.

X-ray diffraction measurements show [3] that the successive layers of Cu and Nb in the composites of interest possess a Kurdjumov–Sachs [10] (KS) orientation relation in

* Corresponding author.
E-mail address: demkowicz@lanl.gov (M.J. Demkowicz).

0022-3115/$ - see front matter © 2007 Elsevier B.V. All rights reserved.
doi:10.1016/j.jnucmat.2007.02.001

which incommensurate interfaces form along the close-packed planes of Cu and Nb ((1 1 1) and (1 1 0), respectively) and the Cu and Nb layers are oriented with respect to each other such that a $\langle 1\,1\,0\rangle$ direction of Cu is parallel to a $\langle 1\,1\,1\rangle$ direction of Nb in the interface plane. Knowledge of the overall crystallographic orientations of Cu and Nb in the multilayer composites, however, is not by itself sufficient to describe the details of atomic arrangement at the interfaces or the physical properties of the interfaces that result from this arrangement.

Misfit strains at incommensurate interfaces have traditionally been thought to be accommodated by arrays of interface dislocations or ledges [11,12]. In the case of some grain boundaries in covalently bonded materials, thin amorphous layers have also been viewed as possible structures for accommodating interface misfit [13,14]. The work presented here describes a third possibility in the case of the Kurdjumov–Sachs interface between Cu and Nb, namely that the interface misfit can be accomodated by a single uniformly strained (1 1 1) monolayer of Cu atoms. Atomistic simulations with embedded atom potentials [15] are used to investigate the relaxed configuration of the proposed structure.

2. Construction of interface configurations

The interfaces under investigation are constructed in a CuNb bilayer. The bilayer is created by joining a (1 1 1) free surface of a slab of perfect fcc Cu containing 17 556 atoms with an appropriately oriented (1 1 0) free surface of a slab of perfect bcc Nb containing 11 016 atoms. The Cu and Nb crystals terminate in free surfaces away from the interface. A total of 21 Cu (1 1 1) planes are stacked normal to the interface plane, giving a Cu layer thickness of 4.4 nm. Stacking 18 Nb (1 1 0) planes gives a total Nb layer thickness of 4.2 nm. These dimensions are comparable to the corresponding layer thicknesses in the CuNb multilayer composites that motivated this study. Furthermore, they are sufficiently large so that – for the atomic force laws used in this study – there are regions in the middle of both the Cu and Nb layers that do not undergo any direct energetic interaction with either the interface plane or the closest free surface. The initial unrelaxed interlayer spacing at the interface is set to the mean of the bulk equilibrium layer spacings between Cu (1 1 1) and Nb (1 1 0) planes, namely 0.221 nm. The CuNb bilayer cross-section parallel to the interface plane is rectangular with dimensions 4.87 nm by 9.71 nm, resulting in an interface area of 47.3 nm^2. Periodic boundary conditions are applied in the interface plane. Because the KS interface between Cu and Nb is incommensurate (it has no exact in-plane periodicity in any direction), ensuring periodic boundary conditions requires the application of a plane strain to one of the adjoining crystal layers: Nb in the case of this study. The shape and dimensions of the Cu and Nb layers are chosen so that this strain is minimized. The values of the strain increments $d\varepsilon_{xx}$, $d\varepsilon_{yy}$, and $d\varepsilon_{xy}$ that must be applied are -0.4%, 0.06%, 0.0%. To determine whether these levels of imposed strain are acceptable for the purpose of determining quantities like differences in interface energy between the interface configurations to be described below, these same configurations are also created in a smaller CuNb bilayer whose dimensions in the interface plane are about one fourth of those corresponding to the larger bilayer described above. The strains imposed to create this small bilayer are $d\varepsilon_{xx} \approx 1.5\%$, $d\varepsilon_{yy} \approx 0.6\%$, $d\varepsilon_{xy} \approx 0.3\%$ and therefore significantly greater than the strains needed create the larger bilayer. The resulting changes in differences between interface energies were around 5 mJ/m^2: an error value that does not affect the conclusions of this study.

Two types of interface structures are considered in this study. The first one – henceforth referred to as KS_1 – is simply the one that results from joining perfect Cu and Nb crystalline layers in the Kurdjumov–Sachs orientation relation as described above. Fig. 1(a) visualizes the relative positions of Cu and Nb interface atoms in a fragment of the KS_1 interface configuration. The positions of individual atoms in this visualization have not been relaxed, but the Cu and Nb crystal slabs were allowed to translate relative to each other until the energy of the composite is minimized with respect to such translations. The second type of interface structure – referred to as KS_2 – is constructed by replacing the Cu (1 1 1) interface plane of the KS_1 struc-

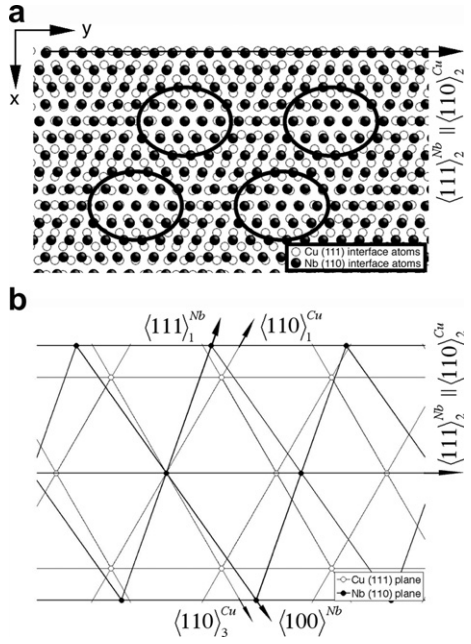

Fig. 1. Visualization (a) of the KS_1 interface configuration looking normal to the interface plane reveals the presence of patches of undercoordination. These patches are identified by circled regions in (a) and occur in the proximity of locations where an interface Cu and Nb atom are positioned nearly 'on top' of each other. The long arrow indicates the characteristic KS direction where $\langle 1\,1\,1\rangle_2^{Nb} \| \langle 1\,1\,0\rangle_2^{Cu}$. The relative orientations of rows of interface Cu and Nb atoms lying along low-index directions are shown in (b). The magnitude of the Nb lattice constant in (b) has been magnified by about 8% to exaggerate the differences in the interface crystallography.

ture with a monolayer of Cu atoms whose construction is described below.

Consider the arrangement of rows of atoms lying along low-index directions in the interface Cu and Nb planes of the KS_1 configuration, as shown in Fig. 1(b). In the Cu (1 1 1) interface plane, close-packed atom rows lie along three possible $\langle 1\,1\,0\rangle$ directions, labeled $\langle 1\,1\,0\rangle_1^{Cu}$, $\langle 1\,1\,0\rangle_2^{Cu}$, and $\langle 1\,1\,0\rangle_3^{Cu}$ in Fig. 1(b). In the Nb (1 1 0) interface plane, close-packed atom rows lie along two possible $\langle 1\,1\,1\rangle$ directions – labeled $\langle 1\,1\,1\rangle_1^{Nb}$ and $\langle 1\,1\,1\rangle_2^{Nb}$ in Fig. 1(b) – while the second-closest packed rows of atoms lie along the $\langle 1\,0\,0\rangle$ direction, labeled $\langle 1\,0\,0\rangle^{Nb}$ in Fig. 1(b). To create the strained Cu monolayer used in constructing the interface arrangement KS_2, a homogeneous in-plane deformation is applied to a Cu (1 1 1) plane such that the close-packed rows $\langle 1\,1\,0\rangle_1^{Cu}$, $\langle 1\,1\,0\rangle_2^{Cu}$, and $\langle 1\,1\,0\rangle_3^{Cu}$ are transformed into a new set of monolayer atom rows named A, B, and C, respectively. These monolayer rows satisfy the following conditions:

1. The direction of monolayer rows A is parallel to the direction of $\langle 1\,1\,0\rangle_1^{Cu}$.
2. The direction of monolayer rows C is parallel to the direction of $\langle 1\,0\,0\rangle^{Nb}$.
3. The distance $d(A)$ between atoms along monolayer rows A is chosen such that the perpendicular spacing $s(C)$ between rows of monolayer atoms lying along the directions of C rows is equal to the perpendicular spacing $s(\langle 1\,0\,0\rangle^{Nb})$ between Nb $\langle 1\,0\,0\rangle^{Nb}$ rows.
4. The distance $d(C)$ between atoms along monolayer rows C is chosen such that the perpendicular spacing $s(A)$ between rows of monolayer atoms lying along the directions of A rows is equal to the perpendicular spacing $s(\langle 1\,1\,0\rangle_1^{Cu})$ between Cu $\langle 1\,1\,0\rangle_1^{Cu}$ rows.

The orientation of monolayer directions A, B, and C with respect to the low-index directions in the Cu (1 1 1) and Nb (1 1 0) interface planes is illustrated in Fig. 2(c).

For the monolayer design described above, the distances $d(A)$ and $d(C)$ of atoms lying along monolayer directions A and C may be calculated in terms of the bulk equilibrium cubic lattice constants of Cu and Nb as

$$d(A) = a_{Nb}\frac{2\sqrt{3}}{2+\sqrt{6}} \approx 0.257\ \text{nm},$$
$$d(C) = a_{Cu}\frac{3}{2+\sqrt{6}} \approx 0.244\ \text{nm}. \quad (1)$$

Here, $a_{Cu} = 0.3615$ nm and $a_{Nb} = 0.3301$ nm are used [16]. On the basis of this complete description of the geometry of the as-constructed Cu monolayer, the in-plane deformation that must be imposed on an undistorted Cu (1 1 1) plane to create a monolayer of this type can be calculated. In the A monolayer direction, a tensile strain $\varepsilon_{AA} = \left(\frac{2\sqrt{6}}{2+\sqrt{6}}\right)\cdot\left(\frac{a_{Nb}}{a_{Cu}}\right) - 1 \approx 0.0053$ is required. No strain is required normal to the A monolayer direction. A pure shear strain of $\gamma_{xy} = \frac{2+\sqrt{2/3}-\sqrt{6}}{\sqrt{3}+\sqrt{2}} \approx 0.116$ (equivalent to a symmetric shear strain of $\gamma/2 \approx 0.058$ plus a rotation of 3.34°) completes the transformation. Note that the tensile strain along A monolayer atom rows depends on the ratio of the Cu and Nb lattice constants and implies a decrease of the in-plane density of Cu atoms in the monolayer by about 1 atom for every 188 atoms in a perfect Cu (1 1 1) plane. The pure shear strain, however, does not affect the in-plane atomic density, is independent of the Cu and Nb lattice constants, and results directly from the KS orientation relation.

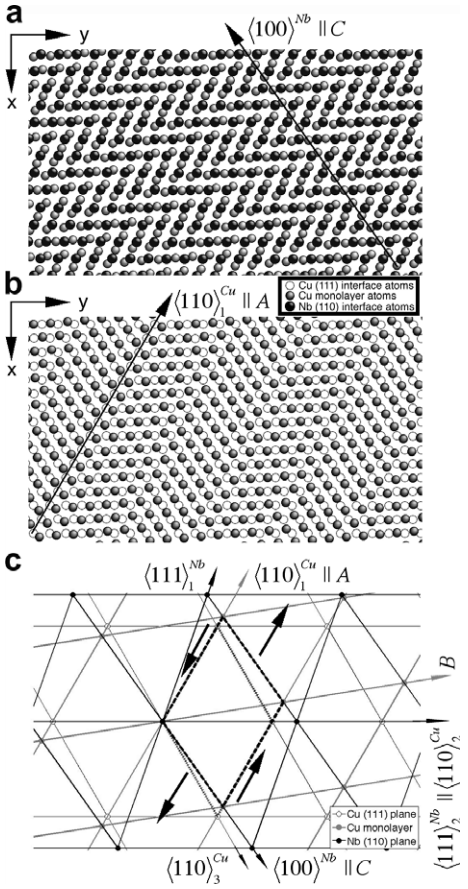

Fig. 2. This figure shows the relative positions of atoms in the strained Cu monolayer (a) with respect to atoms of the Nb (1 1 0) interface plane and (b) with respect to atoms in the Cu (1 1 1) plane that neighbors on the strained Cu monolayer. The viewing direction is normal to the interface plane. Unlike KS_1 (Fig. 1), the KS_2 configuration does not exhibit patches of undercoordination. The long arrows represent monolayer directions A and C in (a) and (b), respectively. The relative orientations of rows of atoms lying along low-index directions in Cu (1 1 1) and Nb (1 1 0) planes as well as rows A, B, and C of the strained Cu monolayer are shown in (c). The magnitude of the Nb lattice constant in (c) has been magnified by about 8% to exaggerate the differences in the interface crystallography. The interfacial Cu monolayer can be constructed by straining a Cu (1 1 1) plane such that monolayer direction A is parallel to direction $\langle 1\,1\,0\rangle_1^{Cu}$ and monolayer direction C is parallel to direction $\langle 1\,0\,0\rangle^{Nb}$. The distance between atoms lying along monolayer rows A is chosen such that the spacing of C rows is equal to the spacing of $\langle 1\,0\,0\rangle^{Nb}$ rows. The distance between atoms lying along monolayer rows C is chosen such that the spacing of A rows is equal to the spacing of $\langle 1\,1\,0\rangle_1^{Cu}$ rows. The straining operations necessary to produce these changes – a uniaxial extension and a pure shear (see text) – are illustrated schematically in (c) by the thick black arrows.

The interface structure KS_2 was created by inserting the Cu monolayer constructed according to the procedure described above in place of the interface Cu (1 1 1) plane of the KS_1 structure. Similarly to when the fcc Cu and bcc Nb crystal slabs are joined to create KS_1, the Cu monolayer inserted to create KS_2 had to be strained to ensure periodic boundary conditions in the interface plane. The required additional plane strain increments $d\varepsilon_{xx}$, $d\varepsilon_{yy}$, $d\varepsilon_{xy}$ are 0.2%, −0.004%, −0.05%, respectively. These strains are smaller than those that relate the Cu monolayer to a perfect Cu (1 1 1) plane and are comparable in magnitude to the strains originally imposed on the bulk Nb to ensure periodic boundary conditions. The resulting interfacial monolayer contains 6 atoms fewer than the original perfect Cu (1 1 1) plane, in agreement with the final level of strain that relates the two planar configurations. For a section of the KS_2 interface configuration, Fig. 2(a) visualizes the positions of Cu atoms in the monolayer with respect to the positions of atoms in the interface (1 1 0) plane of Nb while Fig. 2(b) visualizes the positions of Cu atoms in the monolayer with respect to the positions of atoms in the unstrained (1 1 1) plane of Cu adjoining the monolayer. As in Fig. 1(a), the positions of individual atoms visualized in Fig. 2(a) and Fig. 2(b) have not been relaxed, but the Cu and Nb crystal slabs as well as the strained Cu monolayer were allowed to translate relative to each other until the energy of the composite is minimized with respect to such translations. Note that although none of the monolayer directions *A*, *B*, or *C* lies parallel to the characteristic KS direction where a $\langle 1\,1\,1\rangle$ Nb row is parallel to a $\langle 1\,1\,0\rangle$ Cu row (in Fig. 2(c) row *B* makes an angle of approximately 5.0° with this direction), the overall KS orientation relation is nevertheless preserved between the adjoining Cu and Nb crystals, since neither of them has been distorted or rotated in the course of creating interface structure KS_2.

Given the elastic constants [17] of fcc Cu and the above-calculated values of plane strain increments applied to a Cu (1 1 1) plane, linear elasticity may be used to make an estimate of the order of magnitude of the average energy per atom necessary to create the interfacial Cu monolayer in configuration KS_2. Using the atomic volume of equilibrium fcc Cu, this energy is found to be about 0.03 eV/atom (84.3 mJ/m^2). Since this strain energy may be viewed as an energy penalty associated with the creation of KS_2 from KS_1, one is prompted to ask what characteristic of the KS_2 configuration could offset this energy penalty. The answer can be found by comparing the atomic coordinations in the interface atomic arrangements of KS_1 and KS_2 visualized in Figs. 1(a), 2(a) and (b).

The coordination of an atomic site is determined by counting up all atoms within a cutoff radius of 0.31 nm of that atomic site. This cutoff radius value is chosen because it is larger than the nearest neighbor distances but smaller than the second-nearest neighbor distances in both fcc Cu and bcc Nb at their equilibrium lattice constants. The KS_1 configuration shown in Fig. 1(a) contains distinct patches where interface atoms of Cu and Nb have low coordination. The total coordination of Nb interface atoms in these 'patches of undercoordination' is 7 or 8 while that of Cu atoms is 10. In the KS_2 configuration in Fig. 2(a) and (b), however, the average coordination of Nb interface atoms, Cu monolayer atoms, and atoms in the Cu (1 1 1) plane that adjoins the interfacial Cu monolayer is homogeneous across the entire interface area and equal to approximately 8.5, 10.8, and 12 (respectively). In particular, no patches of undercoordination exist for this interface structure.

In KS_1, patches of undercoordination occur at points where a Cu and Nb atom are positioned such that one is nearly 'on top' of the other. The ubiquity of this feature in incommensurate interfaces has served as the basis for models of interface structure that involve arrays of ledges and dislocations [11,12]. In the KS_2 interface structure, however, the conditions placed on the directions and spacing of monolayer rows *A* and *C* (Fig. 2(c)) guarantee that this 'atom-on-atom' situation never occurs between a monolayer atom and any of the atoms in the Cu (1 1 1) or Nb (1 1 0) planes adjoining the monolayer. Since the direction and spacing between *A* monolayer rows exactly matches those of $\langle 1\,1\,0\rangle_1^{Cu}$ rows, the former will always lie in the 'valleys' between the latter. Similarly, *C* monolayer rows always lie in the 'valleys' between $\langle 1\,0\,0\rangle^{Nb}$ rows. Consequently, no patches of undercoordination exist in the KS_2 interface structure even if the interface is extended infinitely in both in-plane directions.

3. Relaxation of interface configurations

The consequences of the differing initial coordination states of the KS_1 and KS_2 interface structures are investigated by relaxing these structures subject to forces and stresses derived from empirical interatomic potentials and using conjugate gradient energy minimization. The interatomic potentials used in this study are constructed based on the embedded-atom method (EAM) [15], which augments a two-body energetic interaction with an embedding energy computed on the basis of an empirical electron density. This approach has proven successful in modeling properties of elemental metallic systems as well as their alloys [18].

The CuNb potentials used in this study are constructed by adopting the EAM potentials created separately for Cu by Voter [19,20] and for Nb by Johnson and Oh [21]. Since no significant ionic or directional covalent bonding is expected to be present between Cu and Nb, the interaction potentials designed to model bonding between these two elements are based on the usual form used for other metal pairs [20]. Specifically, a two-body Morse interaction potential $\phi_{CuNb}(r)$ is constructed where

$$\phi_{CuNb}(r) = D_M(1 - e^{\alpha_M(r-R_M)}) - D_M, \tag{2}$$

r is the interatomic distance (between a Cu and a Nb atom in the case of $\phi_{CuNb}(r)$), and D_M, α_M, R_M are three fitting constants. A cutoff distance r_{cut} for direct two-body inter-

action between Cu and Nb is implemented by modifying $\phi_{\mathrm{CuNb}}(r)$ so that the numerical value of the modified function $\phi'_{\mathrm{CuNb}}(r)$ as well as of its first derivative are zero at the desired interatomic separation:

$$\phi'_{\mathrm{CuNb}}(r) = \phi_{\mathrm{CuNb}}(r) - \phi_{\mathrm{CuNb}}(r_{\mathrm{cut}}) + \left(\frac{r_{\mathrm{cut}}}{m}\right)\left[1 - \left(\frac{r}{r_{\mathrm{cut}}}\right)^{m}\right]\left(\frac{\mathrm{d}\phi_{\mathrm{CuNb}}}{\mathrm{d}r}\right)_{r=r_{\mathrm{cut}}}. \quad (3)$$

The cutoff distance r_{cut} is a fourth fitting parameter. Two more fitting parameters g_{Cu} and g_{Nb} are obtained by noting that the single-element potentials for Cu and Nb are not affected by the transformation,

$$F'_x(\bar{\rho}) = F_x(\bar{\rho}) + g_x\bar{\rho}, \qquad \phi'_{xx}(r) = \phi_{xx}(r) - 2g_x\rho_x(r) \quad (4)$$

but that the interaction of Cu and Nb is affected by this transformation. Similarly, the transformation,

$$\rho'_x(r) = s_x\rho_x(r), \qquad F'_x(\bar{\rho}) = F_x(\bar{\rho}/s_x) \quad (5)$$

yields a seventh fitting parameter s_{Nb} while $s_{Cu} \equiv 1$ without loss of generality. In the equations above, $F_x(\bar{\rho})$, $\rho_x(r)$, $\bar{\rho}$, and $\phi_{xx}(r)$, respectively refer to the embedding function, electron density function, total electron density at a given atom site, and two-body interaction for element x. See Ref. [17] for more details concerning the functional forms described above.

The construction of EAM interaction potentials for pairs of metal elements is typically accomplished by fitting the corresponding values of dilute enthalpies of mixing [22] and/or the experimentally determined properties of intermetallic phases formed by these elements [23]. Since the immiscible CuNb system does not posses any intermetallic phases, however, the interaction potentials were instead constructed based on the dilute enthalpies of mixing obtained from analytical fitting of the CuNb phase diagram [24] as well as the lattice constant and bulk modulus of a hypothetical CuNb crystal in the CsCl structure obtained by first-principles calculations using VASP [25,26]. Because the interaction term of the EAM potential has seven adjustable parameters [20], however, several different potential parameterizations are possible that give good agreement with the four quantities mentioned above. Because EAM potentials are especially capable of capturing the dependence of atom energies on atom coordinations [27], in this study the excess fitting parameters are used to construct potentials with differing average cohesive energies E_{coh} of CuNb in the NaCl structure, the ZnS structure, and a single sheet of the BN structure. Since in these configurations every Cu (Nb) atom has 6, 4, and 3 Nb (Cu) nearest neighbors, respectively, the dependence of E_{coh} on coordination can be described by a function $E_{\mathrm{coh}} = E_{\mathrm{coh}}(C)$ where C is the atomic coordination. For all potentials constructed, this function is well approximated by the linear equation $E_{\mathrm{coh}} = m \cdot C + b$. The energetic preferability of differently coordinated states can then be summarized by the slope m, more negative values of m indicating a greater preference for atomic environments with higher coordination of Cu by Nb and vice versa. A total of four EAM potentials with interaction terms giving different values of m are constructed. The fitted properties of the interaction terms of these potentials are summarized in Table 1.

Relaxation of the two interface structures with the four CuNb EAM potentials constructed for this study is undertaken in two steps. First, the neighboring crystalline Cu and Nb layers are allowed to translate with respect to each other as rigid bodies, allowing them to assume the most favorable relative positions and interface spacing. In the case of the KS_2 interface, the interfacial Cu monolayer is allowed to undergo independent rigid body translation. The stresses in the CuNb bilayer composites are relaxed to zero by allowing the shapes of the simulation cells to change, though it must be emphasized that this procedure only relaxes the total stress of the composite and that residual stresses arising from the strains required to impose periodic boundary conditions – previously described – remain present in the constituent Cu and Nb layers as well as in the interfacial Cu monolayer, in the case of KS_2. The interface structures thus relaxed are called reference structures because the energies and coordinations determined on their basis describe the interface configurations in their as-constructed or 'reference' states. The interface atomic configurations visualized in Figs. 1 and 2 correspond to such reference states.

In the second relaxation step, all atomic positions are allowed to change independently until the maximum force acting on any atom in the system does not exceed 1.6 pN. In both of the two interface configurations, this relaxation process causes the interface atoms to undergo small-scale displacements characteristic of these atoms' sinking into their nearest equilibrium positions. In no instance, however, were these displacements large enough to constitute a reconstruction of the interface configurations, confirming

Table 1
Fitted properties of the EAM interaction potentials used in this study

Source of numerical values	dH(Nb in Cu) (eV)	dH(Cu in Nb) (eV)	a_{CsCl} (nm)	B_{CsCl} (GPa)	$E_{\mathrm{coh}}^{\mathrm{NaCl}}$ (eV)	$E_{\mathrm{coh}}^{\mathrm{ZnS}}$ (eV)	$E_{\mathrm{coh}}^{\mathrm{BN}}$ (eV)	m (eV)
EAM 1	1.01	0.49	3.24	173	−4.42	−3.59	−3.28	−0.38
EAM 2	1.02	0.50	3.23	175	−4.46	−3.62	−3.30	−0.39
EAM 3	1.00	0.51	3.22	176	−4.51	−3.65	−3.33	−0.40
EAM 4	1.02	0.48	3.31	168	−4.53	−3.65	−3.33	−0.41
Experiment/VASP	1.02 [24]	0.48 [24]	3.22	168	N/A	N/A	N/A	N/A

that both the KS_1 and KS_2 interface structures are at least metastable for the potentials used in this study. In particular, relaxation does not remove the patches of low coordination present in KS_1 (Fig. 1(a)), confirming that they are intrinsic features of this interface structure and do not result from the details of bonding across the interface. The relaxation process, however, does result in a readjustment of the average spacing normal to the interface between successive Cu and Nb planes. Furthermore, elastic in-plane distortions – evidenced by nonhomogeneous atomic displacement fields – are observed in the interface planes themselves. The effect of these distortions is to increase the average coordination of atoms at the interface at the expense of a buildup in the average local atomic-level virial stresses in neighboring regions.

Comparison of the interface energies for the KS_1 and KS_2 configurations in both their reference and fully relaxed states is achieved by evaluating the quantity,

$$\Delta E_{\text{int}} = V_{\text{KS}_2} - (V_{\text{KS}_1} - 6 \cdot E_{\text{coh}}^{\text{Cu}}), \tag{6}$$

where V_{KS_1} and V_{KS_2} are the potential energies of CuNb bilayers containing KS_1 and KS_2 interface structures, respectively, and $E_{\text{coh}}^{\text{Cu}} = -3.54$ eV/atom is the cohesive energy of fcc Cu. As discussed previously, the KS_2 interface configuration examined in this study contains 6 Cu atoms fewer than the KS_1. This difference must be taken into account when comparing the energies of the two interface structures by subtracting 6 times the cohesive energy of Cu from the KS_1 energy. This method of accounting can be understood through the thought experiment of creating 6 vacancies in the KS_1 structure, allowing them to migrate to the interface with Nb, and then reconstructing the interface Cu layer into the structure posited for the interfacial Cu monolayer in the KS_2 configuration. The quantity ΔE_{int} can also be evaluated plane-by-plane for atomic planes parallel to the interfaces. Doing so confirms that the overall value of ΔE_{int} arises from energy differences only in the vicinity of the interface: by far the largest contributions come from the Cu plane and Nb plane that lie adjacent to each other while contributions from planes beyond two nearest neighbor distances from the interface are zero.

Fig. 3 shows the differences in interface energies ΔE_{int} and the average coordinations $\langle C \rangle^{\text{Cu}}$ and $\langle C \rangle^{\text{Nb}}$ of atoms in interface Cu and Nb planes as a function of m for the reference and relaxed configurations of the KS_1 and KS_2 interface structures. For KS_1, $\langle C \rangle^{\text{Cu}}$ refers to the Cu (1 1 1) plane that neighbors on the nearest plane of Nb atoms while in KS_2 it refers to the strained interfacial Cu monolayer. In both KS_1 and KS_2, $\langle C \rangle^{\text{Nb}}$ refers to the Nb (1 1 0) plane that neighbors on the nearest plane of Cu atoms. The reference interface energy difference clearly favors the KS_2 structure (Fig. 3(a)), indicating that the elastic energy penalty associated with creating the strained Cu monolayer is more than adequately made up for by the increased average coordination state of atoms in both the interfacial Cu monolayer (Fig. 3(b)) and the Nb interface (1 1 0) plane (Fig. 3(c)). The average coordination of Cu atoms in the (1 1 1) plane immediately adjoining the interfacial Cu monolayer in KS_2 in both the reference and fully relaxed structures is nearly constant (independent of m) and equal to approximately 11.98, indicating that the presence of the interfacial Cu monolayer does not significantly reduce the coordination state of the adjoining Cu atoms while significantly increasing the coordination state of interface Cu and Nb atoms over the KS_1 structure.

When the KS_2 interface is fully relaxed, the average coordination of its interface atoms increases by an increment that is independent of the measure of energetic preference m given to differing CuNb coordinations. On the other hand, the increase of average coordinations of inter-

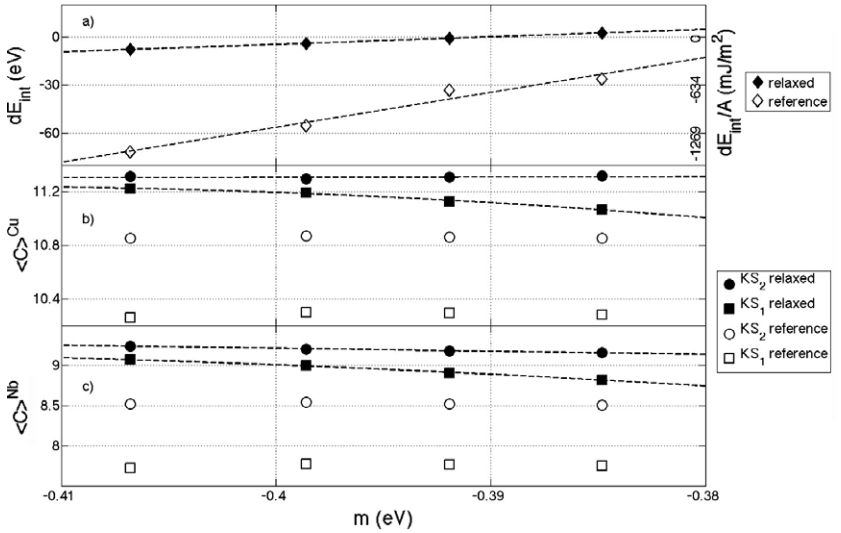

Fig. 3. (a) The KS_2 interface configuration becomes increasingly energetically favorable compared with the KS_1 configuration as the measure m of preference for higher coordination states (see text) becomes more negative. This trend is caused by the higher coordination state of interface atoms in the KS_2 configuration on both the (b) Cu and (c) Nb sides and for both the reference and relaxed configurations.

face atoms in the KS_1 structure is both larger than in the KS_2 case and strongly dependent on the value of m (Fig. 3(b) and (c)). More negative values of m (which favor higher coordinations) result in greater increases in coordination. Consequently, for decreasing values of m, the average coordinations of interface atoms in the KS_1 structure appear to asymptotically approach the average coordination values of the KS_2 structure. On this basis, one might be led to believe that the energy difference between the relaxed KS_1 and KS_2 interface structures would be eventually reduced to zero as m decreases. Fig. 1(a), however, clearly shows that this is not the case: ΔE_{int} decreases with decreasing m, as it does in the case of the reference KS_1 and KS_2 interface structures. This similarity in the dependence of ΔE_{int} on m for both the reference and relaxed interface structures – despite the convergence of $\langle C\rangle^{\text{Cu}}$ and $\langle C\rangle^{\text{Nb}}$ with decreasing m in the latter – stems from the energy penalty associated with the buildup of virial stresses in the relaxed KS_1 interface in regions neighboring the interface: a buildup that is necessary to accommodate the increase in average coordination.

4. Discussion

The arguments presented above demonstrate that an elastically strained interfacial monolayer may lead to an energetically favorable interface structure compared to one formed as a result of joining two crystal lattices despite the elastic energy penalty associated with its creation. This possibility exists because the presence of the monolayer improves the coordination state of atoms at the interface. Thin layers of interfacial material have been proposed previously in the contexts of two-phase mixtures near their critical point [28,29] and of formation of amorphous interfacial layers in interfaces between materials with highly directional covalent bonding [13,14]. The interfacial atomic Cu monolayer proposed in this study differs from both of these cases in that it is not amorphous and does not require directional bonding or high temperatures to enable its stability.

Because accurate determination of relative energies of incommensurate interface structures requires systems composed of thousands of atoms (otherwise the strain energies associated with imposing periodic boundary conditions would dramatically skew the results), first principles methods are not likely to provide conclusive evidence concerning whether interface structures containing interfacial monolayers such as KS_2 are energetically preferable to ones like KS_1. Direct HRTEM observations along close-packed atomic rows parallel to the interface plane would furnish more compelling demonstrations.

As pointed out in Section 1, given the superior radiation damage resistance made possible by interfaces in CuNb multilayer composites [6,7], the ability to predict what other pairs of materials are capable of supporting interfacial monolayers could be of great technological value in selecting materials for next generation nuclear reactors. Although presently such predictions cannot be made with certainty, the insight gained from studying the structure of CuNb interfaces suggests two simple principles whose application can significantly narrow the number of likely candidate element pairs. These principles are:

1. The pair of materials should be immiscible. Otherwise, the materials would tend to interdiffuse, preventing the formation of atomically sharp interfaces.
2. The lattice constants of the materials forming the interface should predict strains associated with creating an interfacial monolayer that are on the order of the strains necessary in the CuNb system, or smaller. Otherwise, the resulting elastic energy penalty for creating a strained interfacial monolayer would be increased.

The strains mentioned in principle 2 may be easily found for Kurdjumov–Sachs interfaces between fcc and bcc element pairs using the expression for ε_{AA} stated before if the equilibrium lattice constants for the elements are known [16]. Excluding all element pairs with ε_{AA} values above 0.01, one obtains six candidate pairs out of a possible 255, namely: CaBa, ThEu, IrLi, PdLi, CuNb, and CuTa. Of these, only CuNb and CuTa are know to be immiscible [30] (no miscibility data could be found for CaBa and ThEu). This result suggests that the conditions necessary for constructing interfacial monolayers are not common and that the choice to study the properties of CuNb was rather fortuitous. Nevertheless, Kurdjumov–Sachs interfacial monolayer designs other than the one described here are certainly possible as are designs for different interface types, such as ones obeying the Nishiyama–Wasserman [31,32] orientation relation. Finally, the search need not be limited to fcc–bcc element pairs or to pure elements. An extensive listing of material pairs whose interfaces are likely candidates for forming interfacial monolayers as well as a description of point defect behavior near such interfaces will be presented elsewhere.

In summary, an atomic configuration has been proposed for the Kurdjumov–Sachs (KS) interface between Cu and Nb where the misfit between the adjoining crystals is accommodated by an atomic monolayer of Cu. This monolayer can be described as a perfect Cu (1 1 1) plane that has been strained in such a way as to remove patches of undercoordination present in a KS interface created by simply joining two perfect Cu and Nb crystals. Although an elastic energy penalty is associated with such straining, the improved coordination of interface atoms can stabilize the interface configuration containing an interfacial Cu monolayer. Two principles are proposed for selecting pairs of candidate materials other than CuNb that are likely to exhibit interface structures containing strained monolayers.

Acknowledgements

We thank A. Misra, Srinivasan G. Srivilliputhur, Y.-C. Wang, N. A. Mara, M. I. Baskes, and R. B. Schwarz for

many stimulating discussions. The atomic structure visualizations presented here were generated using the AtomEye program [33]. This work was supported by the U.S. Department of Energy Office of Basic Energy Sciences' Division of Materials Sciences, the Los Alamos National Laboratory Directed Research and Development Program, and a Los Alamos director's funded postdoctoral fellowship.

References

[1] A. Misra, R.G. Hoagland, H. Kung, Phil. Mag. 84 (2004) 1021.
[2] A. Misra, R.G. Hoagland, J. Mat. Res. 20 (2005) 2046.
[3] P.M. Anderson, J.F. Bingert, A. Misra, J.P. Hirth, Acta Mater. 51 (2003) 6059.
[4] A. Misra, H. Kung, D. Hammon, R.G. Hoagland, M. Nastasi, Int. J. Damage Mech. 12 (2003) 365.
[5] Y.C. Wang, A. Misra, R.G. Hoagland, Scripta Mater. 54 (2006) 1593.
[6] T. Hochbauer, A. Misra, K. Hattar, R.G. Hoagland, J. Appl. Phys. 98 (2005) 123516.
[7] M.J. Demkowicz, Y. Wang, R.G. Hoagland, and O. Anderoglu, Nuc. Inst. Meth. B, in press.
[8] E. Snoeck, F. Lecouturier, L. Thilly, M.J. Casanove, H. Rakoto, G. Coffe, S. Askenazy, J.P. Peyrade, C. Roucau, V. Pantsyrny, A. Shikov, A. Nikulin, Scripta Mater. 38 (1998) 1643.
[9] L. Thilly, M. Veron, O. Ludwig, F. Lecouturier, Mat. Sci. Eng. A 309&310 (2001) 510.
[10] G.V. Kurdjumov, G. Sachs, Z. Phys. 64 (1939) 325.
[11] M.G. Hall, H.I. Aaronson, K.R. Kinsma, Surf. Sci. 31 (1972) 257.
[12] J.M. Rigsbee, H.I. Aaronson, Acta Metall. 27 (1979) 351.
[13] P. Keblinski, S.R. Phillpot, D. Wolf, H. Gleiter, Phys. Rev. Lett. 77 (1996) 2965.
[14] P. Keblinski, S.R. Phillpot, D. Wolf, H. Gleiter, Acta Mater. 45 (1997) 987.
[15] M.S. Daw, M.I. Baskes, Phys. Rev. B 29 (1984) 6443.
[16] D.E. Gray, American Institute of Physics Handbook, McGraw-Hill, New York, 1957.
[17] G. Simmons, H. Wang, Single Crystal Elastic Constants and Calculated Aggregate Properties: A Handbook, MIT, Cambridge, MA, 1971.
[18] M.S. Daw, S.M. Foiles, M.I. Baskes, Mat. Sci. Rep. 9 (1993) 251.
[19] Y. Mishin, M.J. Mehl, D.A. Papaconstantopoulos, A.F. Voter, J.D. Kress, Phys. Rev. B 63 (2001) 224106.
[20] A.F. Voter, in: J.H. Westbrook, R.L. Fleischer (Eds.), Intermetallic Compounds: Principles and Practice, vol. 1, Wiley, New York, 1994, p. 77.
[21] R.A. Johnson, D.J. Oh, J. Mat. Res. 4 (1989) 1195.
[22] S.M. Foiles, M.I. Baskes, M.S. Daw, Phys. Rev. B 33 (1986) 7983.
[23] A.F. Voter, S.P. Chen, Mat. Res. Soc. Symp. Proc. 82 (1987) 175.
[24] L. Kaufman, Calphad 2 (1978) 117.
[25] G. Kresse, J. Hafner, Phys. Rev. B 47 (1993) 558.
[26] G. Kresse, D. Joubert, Phys. Rev. B 59 (1999) 1758.
[27] M.I. Baskes, S.G. Srinivasan, S.M. Valone, and R.G. Hoagland, Phys. Rev. B, in press.
[28] J.W. Cahn, J. Chem. Phys. 66 (1977) 3667.
[29] E.I. Rabkin, L.S. Shvindlerman, B.B. Straumal, Int. J. Mod. Phys. B 5 (1991) 2989.
[30] F.R. de Boer, R. Boom, W.C.M. Mattens, A.R. Miedema, A.K. Niessen, Cohesion in Metals: Transition Metal Alloys, North-Holland, Amsterdam, 1988.
[31] Z. Nishiyama, Sci. Rept. Tohoku Univ. 23 (1934) 368.
[32] G. Wasserman, Arch. Eisenhuttenwesen 16 (1933) 647.
[33] J. Li, Mod. Sim. Mat. Sci. Eng. 11 (2003) 173.